Assessing the Influence of Grid-Connected PV Systems on Algeria's Low Voltage Distribution Network

Madjid Chikh[1*] iD **, Aicha Degla[2]** iD **, Smain Berkane[1a]** iD **, Achour Mahrane[1b]** iD **,**

Abdalbaset Mnider[3,4] iD *.*

[1] Le Commissariat aux *énergies renouvelables et à l'efficacité énergétique* (CEREFE),
B.P.23, Docteur Asselah Slimane, Alger Centre 16000.
[1*,1a,1b]Unité de Développement des Equipements Solaires UDES, Algiers, Algeria,
Route nationale N 11, BP 386, Boui-Smail, 42415, wilaya de Tipaza.
[2]Centre de Development des Energies Renouvelables CDER, Algiers, Algeria,
B.P. 62, Route de l'Observatoire Bouzaréah, 16340, Alger, Algérie.
[3]Dept. of Electronic & Electrical Eng University of Strathclyde Bahrain, Manama, Bahrain.
[4]Elmergib University AlKhums, Libya

E-*mail:* [1*] *m.chikh@cerefe.gov.dz*

ARTICLE INFO.

ABSTRACT

The integration of renewable energy into power systems is a growing area of interest, particularly in regions with high solar potential. This study investigates the impact of a 12.5 kWp multi-technology photovoltaic (PV) power station on the local utility grid. The system comprises five PV arrays using different technologies, installed on the rooftop and façade of the UDES/CDER conference room in Tipaza, Algeria. Experimental data were collected to evaluate the grid voltage variations at the grid-connected point under real operating conditions. Voltage levels remained within the EN 50160 standard limits, with fluctuations typically ranging from 229 V to 236 V.

The total harmonic distortion (THD) of current remained below 5% during peak injection periods, meeting IEC 61000-3-2 standards. Statistical analysis of THD and power factor (PF) distributions for three PV power output levels showed that more than 80% of current THD values were concentrated in the 5–10% range, with standard deviations decreasing as PV output increased. Voltage THD means decreased from 2.42 to 2.26 with rising PV generation, and over 96% of values were well below the EN 15160 limit.

Statistical analysis of THD and power factor (PF) distributions for three PV power output levels showed that more than 80% of current THD values were concentrated in the 5–10% range, with standard deviations decreasing as PV output increased. Voltage THD means decreased from 2.42 to 2.26 with rising PV generation, and over 96% of values were well below the EN 15160 limit. PF values remained strongly clustered around unity for all output levels. Results demonstrate that active PV power injection had a stabilizing effect on the voltage profile during daylight hours, with minimal adverse impact on power quality. These findings highlight the viability of small-scale, multi-technology PV systems for grid integration in similar climatic and infrastructural contexts.

<div dir="rtl">

تقييم أثر أنظمة الطاقة الكهروضوئية المرتبطة بالشبكة على شبكات التوزيع الكهربائية ذات الجهد المنخفض في الجزائر

مجيد شيخ، عائشة دقلة، إسماعين بركان، عاشور مهران، عبد الباسط منيدر

ملخـــص: يجب أن يشكّل إدماج مصادر الطاقة المتجددة في أنظمة القوى الكهربائية مجالاً متنامياً للاهتمام، ولا سيما في المناطق ذات الإمكانات الشمسية المرتفعة. تهدف هذه الدراسة إلى تحليل أثر محطة كهروضوئية متعددة التقنيات بقدرة 12.5 كيلوواط ذروة على شبكة التوزيع الكهربائية المحلية. يتكون النظام من خمس حقول كهروضوئية تستخدم تقنيات مختلفة، تم تركيبها على سطح وواجهة قاعة المؤتمرات التابعة لوحدة تطوير الأجهزة الشمسية/المركز الوطني لتطوير الطاقات المتجددة في تيبازة، الجزائر. وقد جُمعت بيانات تجريبية لتقييم تذبذبات الجهد الكهربائي عند نقطة الربط مع الشبكة تحت ظروف تشغيل فعلية. أظهرت النتائج أن مستويات الجهد بقيت ضمن حدود المعيار الأوروبيEN 50160 ، حيث تراوحت غالباً بين 229 و236 فولت. كما ظل التشوه التوافقي الكلي للتيار أقل من 5% أثناء فترات الحقن القصوى، متوافقاً مع متطلبات المعيار IEC 61000-3-2. وأبان التحليل الإحصائي لتوزيع قيم التشوه التوافقي الكلي ومعامل القدرة عند ثلاثة مستويات مختلفة من إنتاج الطاقة الكهروضوئية أن أكثر من 80% من قيم التشوه التوافقي الكلي للتيار تركزت في المجال 5–10%، مع انخفاض الانحراف المعياري بارتفاع الإنتاج. كما انخفض متوسط التشوه التوافقي الكلي للجهد من 2.42 إلى 2.26 مع زيادة التوليد الشمسي، في حين أن أكثر من 96% من القيم ظلت دون الحد المسموح به في المعيار EN 15160. أما قيم معامل القدرة فقد بقيت متمركزة بقوة حول الوحدة في جميع مستويات الإنتاج. وتبيّن النتائج أن الحقن النشط للطاقة الكهروضوئية أسهم في استقرار منحنى الجهد خلال ساعات النهار، مع تأثيرات سلبية طفيفة للغاية على جودة القدرة. وتؤكد هذه النتائج جدوى دمج الأنظمة الكهروضوئية صغيرة السعة ومتعددة التقنيات في الشبكة الكهربائية ضمن ظروف مناخية وبنيوية مشابهة.

</div>

1. INTRODUCTION

The increasing deployment of PV energy systems is reshaping the landscape of electrical power generation worldwide. With global PV capacity reaching 627 GW by 2019, as reported by the International Energy Agency [1], the shift toward grid-connected renewable energy is accelerating. Among renewable technologies, PV is particularly promising due to its cost-effectiveness and the efficiency gains of modern solar cells [2][3]. However, this growth raises several operational challenges for distribution networks, especially concerning power quality and voltage regulation. A significant body of research has examined the technical implications of PV integration into low-voltage (LV) distribution grids. For instance, Canova et al. [4] and Shalwala et al. [5] analyzed the impact of rooftop PV systems on voltage profiles in Italy and Saudi Arabia, respectively, identifying issues such as voltage rise and impedance-induced peaks. Similarly, Gonzalez et al. [6] and Munirah Ayub et al.[7] evaluated harmonic distortions resulting from PV injection, highlighting the potential degradation of power quality. In the Malaysian context, studies by Chin Ho Tie [8] and Ayub et al. [7] showed a correlation between

PV output and voltage imbalance, especially under uneven irradiance or loading conditions. Other researchers have focused on system-level effects, such as reactive power compensation and reverse power flow. Alam et al. [9] emphasized the need for 24-hour monitoring tools to mitigate overvoltages during peak production. Davud Mustafa et al. [10] argued that no absolute upper threshold exists for PV integration; instead, the effects depend heavily on network configuration and PV distribution. Simulation-based studies in Burkina Faso by Guingane et al. [11] showed that high PV injection levels may lead to instability due to overvoltage during mid-day peak radiation. Recent research has evolved toward proposing intelligent control and monitoring solutions. For instance, D. Chathurangi et al. [12] reviewed hosting capacity assessment methods under voltage rise constraints, while Forson Peprah et al. [13] evaluated rooftop PV systems in terms of power quality and voltage stability. Salem et al. [14] focused on harmonic distortions and flicker in LV grids under various PV integration scenarios. Advanced techniques using smart inverters [15], digital twins [16], and probabilistic models [17] have also been proposed to enhance real-time voltage regulation and to anticipate operational costs under PV-EV coupling. While these contributions provide valuable insights, most of them rely on simulation models or single-technology PV setups, often overlooking the effects of multi-technology PV systems operating under real-world environmental conditions, especially in semi-arid or North African climates. Moreover, the variability introduced by façade-mounted versus rooftop-mounted arrays, and the combined influence of irradiance, angle, and temperature, remain underexplored in empirical studies. There is a lack of experimental research evaluating how multi-technology PV systems affect grid voltage and power quality under real conditions. Particularly in the MENA region, where solar potential is high and the infrastructure is still adapting to distributed generation, field data is essential to validate standards and support policy and system design. This paper addresses this gap by analyzing the grid-integration effects of a 12 kWp grid-connected, multi-technology photovoltaic (PV) plant installed at the UDES/CDER conference facility in Tipaza, Algeria. The system comprises five PV arrays employing different technologies and orientations, both rooftop- and façade-mounted, enabling a comparative assessment under diverse solar capture conditions. The objectives of this work are to:

- Evaluate voltage variations at the grid connection point under real operating conditions;
- Measure the THD of current and voltage, as well as the PF, across varying PV output levels;
- Apply statistical analyses (mean, standard deviation, confidence intervals) to characterize the distribution of these parameters;
- Quantitatively compare the results with the limits set by EN 50160 [18] and IEC 61000-4-30 [19] standards.

By combining compliance assessment with statistical modeling, this study provides original, real-world insights into the dynamic interaction between heterogeneous PV modules and the utility grid. The findings not only evaluate the technical feasibility and reliability of such systems but also highlight their potential for stable and standard-compliant integration in developing-country contexts with high solar resources.

This paper is organized as follows: Section 2 provides a detailed description of the experimental PV system and the measurement instruments used. Section 3 outlines the relevant power quality standards that serve as benchmarks for analysis. Section 4 presents and discusses the experimental results, focusing on voltage variation, harmonic distortion, power factor and atatistical analysis. Finally, Section 5 summarizes the key findings and offers practical

recommendations based on the observed system performance.

2 THE MULTI-TECHNOLOGY PV POWER PLANT DESCRIPTION

This study investigates a multi-technology PV power plant connected to the UDES power grid. The plant features a total installed capacity of 12.5 kWp and integrates six PV arrays employing different photovoltaic technologies.

2.1. Physical Layout and Technologies Used

The PV system consists of 78 modules, divided between crystalline and thin-film technologies. Crystalline silicon modules both monocrystalline and multicrystalline are installed on the building's rooftop with a 30° south-facing tilt. In contrast, thin-film modules, including amorphous and micromorphous silicon types, are mounted vertically on the building's façade (see Figure 1(a)). Each PV array has a nominal capacity ranging from 1.4 kWp to 2.3 kWp, as summarized in Table 1. To highlight the technological diversity of the PV plant, Table 1 presents the main characteristics of the five installed photovoltaic subsystems. Each system differs in PV module technology, manufacturer, and inverter type. The configurations include multicrystalline, amorphous, and monocrystalline silicon technologies, with module power ratings ranging from 110 Wp to 185 Wp. The number of modules per array varies from 8 to 20, resulting in nominal capacities between 1.1 kWp and 2.56 kWp. Each subsystem is connected to the grid via a dedicated single-phase inverter from a different manufacturer (SMA, SolarMax, Aurora, and Fronius). This heterogeneous setup offers a robust experimental platform for analyzing the performance, compatibility, and impact on power quality of various PV technologies operating under identical environmental conditions.

(a)   **(b)**

Figure 1 (a) Crystalline silicon PV panels (c-Si, m-Si) on rooftop and thin-film (a-Si, m-Si) on the facade of the UDES building. (b) The control room of the multi-technology PV power plant is connected to the UDES grid.

Table 1. Description of the distributed photovoltaic arrays of the Multi-technology plant.

	Syst 01	Syst 02	Syst 03	Syst 04	Syst 05
Power	*10 modules of 110Wp*	*20 modules of 128Wp*	*20 modules of 110Wp*	*20 modules of 110Wp*	*8 modules of 185Wp*
Technology	*mSi model Kyocera KD140*	*a-Si model SHOT*	*a-Si, model Sharp NAF128*	*c-Si, model Solar23*	*C-Si, model JT Solar*
PV inverter	*SB 1700*	*Solar Max 2000*	*SB 2000*	*Aurora 2000*	*Fronius IG 1500*

2.2. Electrical Configuration and Inverters

Each of the six PV arrays is connected to the electrical grid via individual single-phase inverters. The system employs inverters from different manufacturers, including SMA, Fronius, SolarMax, and Power One. As illustrated in Figure 1(b), the inverters are housed in the technical control room, which also contains the AC and DC power distribution and control

units. The plant's electrical layout, shown in Figure 2, distributes five PV subsystems across three grid phases, with two arrays per phase.
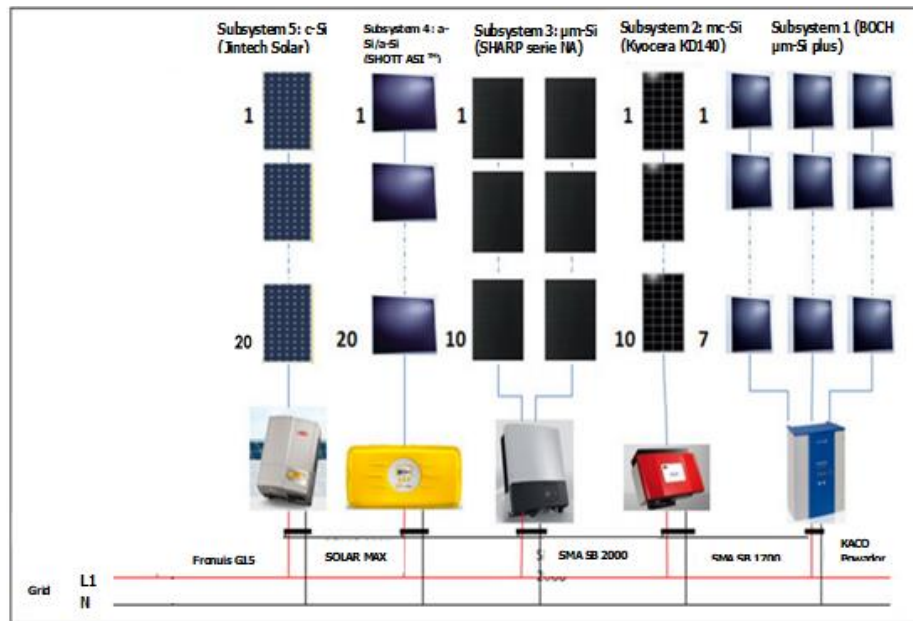

Figure 2. Electrical schematic diagram of the multi-technology photovoltaic power plant.

2.3. Monitoring and Measurement Setup

To analyze the performance and impact of the PV system on power quality, a dedicated monitoring system has been deployed. This system continuously measures critical electrical parameters including voltage at the point of common coupling, inverter output frequency, injected power, power factor, harmonic levels, and THD.

The instrumentation setup includes AC current sensors, a multifunction digital multimeter, a HIOKI 3390 power analyzer, and a data acquisition system, as shown in Figure 3. These devices enable real-time monitoring and analysis of system behaviour under varying weather conditions and operational states.
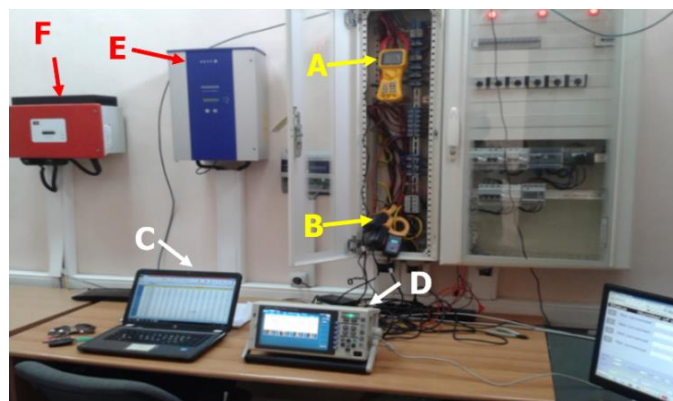

Figure 3. Test and measurement platform in the control room.
(A) Multimeter, (B) Current sensors, (C) Software, (D) Power analyzer, (E) inverter, (F) PV inverter.

2.4. Grid Integration and Evaluation Protocol

The full output of the PV system is injected into the UDES unit's internal power grid, operating in islanding mode. To evaluate the system's influence on grid performance, a custom

experimental protocol has been developed. Given the absence of standardized testing procedures, particular emphasis was placed on the sequencing and timing of measurements to ensure accurate assessment of voltage fluctuations, current variability, and THD during PV-grid interaction.

3. METHODOLOGY

The study aimed to assess the integrity of the energy grid by monitoring voltage, current, and THD in a detached PV system. Measurements were conducted over a period of four months, from March to June, covering the seasonal transition from late winter to early summer in a Mediterranean climate. Electrical data were recorded every 5 minutes using a calibrated power analyzer and data acquisition system. Limited experiments were also conducted at night, with all conference room loads including lighting being active. These nighttime tests served to establish a baseline load profile in the absence of solar input. The PV system sends electricity into a single phase of the electrical grid, and the testing approach was evaluated under three power ranges: low power (0–4.15 kWp), middle power (0–7.25 kWp), and high power (0–12.5 kWp). To ensure consistency, several tests were repeated under similar environmental and load conditions. Weather and solar irradiance were monitored throughout the campaign using a pyranometer installed on-site. Only data collected during stable irradiance periods (e.g., clear skies or consistent overcast conditions) were retained for analysis. The research aimed to examine how PV output variability affects grid quality, focusing on voltage fluctuation, inverter frequency, and harmonic distortions. The collected data allowed an in-depth analysis of how parameter volatility impacts network voltage, particularly with regard to energy quality and regulatory compliance. The study aimed to investigate how the volatility of each recorded parameter impacts network voltage, particularly network energy quality. Reliability of service and adherence to the agreement's voltage and frequency parameters are critical concerns for energy network providers and distributors [23]. Traditional distribution networks have a greater voltage at the substation that supplies power and a lower voltage at the end of the distribution feeder. From the substation of origin, electricity is sent directly to the consumers. However, once THD is present, network activity is triggered and the power transits are fine-tuned. Referring to Figure 4, we can use equation (1) to calculate the voltage drop U along the transmission line between the source substation and the PV power plant.

A simplified theoretical model is presented in Figure 4 to illustrate how the PV system's injected current interacts with the distribution feeder impedance, resulting in voltage variation (ΔV). This conceptual diagram supports the interpretation of voltage fluctuations measured during the experimental campaign.

$$\Delta U = RI_t \cos(\theta) + L\omega I_t \sin(\theta) \qquad (1)$$

Where: R, L are the total resistance and inductance of the line, respectively, It is the current flowing in the line, cos(θ) is the power factor expressed by the following equation.

$$\cos(\theta) = \frac{P_N}{S_N} \qquad (2)$$

Where PN and SN are the active and apparent powers, respectively

$$\Delta U = R\frac{P_N}{U_N} + L\omega\frac{Q_N}{U_N} = \frac{R(P_{PV}-P_L)+L\omega(\pm Q_{PV}-Q_L)}{U_N} \qquad (3)$$

UN voltages at nodes N, PPV, QPV are the active and reactive power plants. PL, QL are the
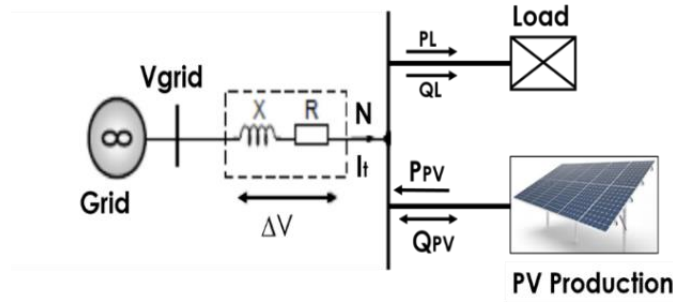
active and reactive powers consumed.

Figure 4. The voltage drops on a line

Equation (4) depicts the main problems associated with connecting a PV power plant to the grid. Indeed, the power injection, active or reactive, will lead to a voltage increase across the grid connection node. The voltage impacts resulting from such products will differ depending on the type of grid to which they are connected. According to the network structure, the source substation characteristics, the connection point, and the power injected by the THD, the voltage at the connection point may be high and may even exceed the permissible limit.

$$\Delta U = \frac{RP_N + XQ_N}{U_N} \tag{4}$$

In the transmission network, the reactance is greater than the resistance, so if X>>R, equations (3 - 4) can be simplified as equation (5):

$$\Delta U = \frac{XQ_N}{U_N} \tag{5}$$

As a result, the voltage level will be affected more by reactive power injection than by active power injection. The linear resistance R>>X is more critical than the linear reactance R>>X in the distribution network, particularly for the low-voltage grid.

$$\Delta U = \frac{RP_N}{U_N} \tag{6}$$

The THD for a voltage (THD, Uac) or the THD for current (THD, Iac) Harmonic distortion is quantified by the waveform [7], which is the total of the voltage or current magnitudes of all harmonic components divided by the amplitude of the fundamental frequency. Equations (7-8) may be used to determine it [4][12]

$$\text{THD}, U_{ac}(\%) = \frac{\sqrt{U_2{}^2 + U_3{}^2 + U_H{}^2}}{U_1} 100 \tag{7}$$

Where U2, U3, UH are the magnitudes of voltage harmonic and U1 is the fundamental voltage.

$$THD, I_{ac}(\%) = \frac{\sqrt{I_2{}^2 + I_3{}^2 + I_H{}^2}}{I_1} 100 \tag{8}$$

In addition, I2, I3, IH are the magnitudes of the current harmonics, and I1 is the fundamental current.

3.1. Power quality standards

Variation in voltage, current, and frequency are often used as indicators of power quality. In this part, we compare the findings of our research to international standards for power quality.

3.1.1. Frequency standards

The frequency of low-voltage grid (230/400 V) electricity is standardized at 50 Hz globally. Assuming that the grid's producing capacity and demand are substantially matched together with no instant rate change in either condition, synchronous generators typically regulate the grid's frequency in power systems built around large-scale distributed power plants. While 50 Hz frequency is recognized globally, Table 2 shows that there are some variances in the upper and lower tolerances across nations under typical operating circumstances. Time tolerances may also vary (e.g., 99.5% under the standard EN 50160[20] but 99% under the standard AS 60038-2012 [21]). These contextual differences are fundamental for any regional frequency analysis.

3.2 Voltage standards at the grid connection point

Table 2. provides a summary of the international standards adopted by various countries. Tolerances of 6% for voltage are used in New Zealand's implementation of the 230V standard, while 10% and 6%, respectively, are preferred in the United Kingdom and Australia. Both of these countries have approved the 230V standard.

Table 2. Comparison of declared supply voltage standards

Country/Region	Allowable Voltage at Customer's Point of Supply	Voltage Range (V)	Frequency range (Hz)	Standard/Regulation/ Reference
Germany	*230 V ±10%*	*207–253*	*49.5–50.5*	*EN50160 [20]*
United Kingdom	*230 V +10%, −6%*	*216.2–253*	*49.5–50.5*	*BS7671[22]*
USA	*120 V ±5%*		*50±0.08 (60Hz)*	*ANSI Standard C84-1 (2016)[23]*
New Zealand	*230 V ±6%*		*49.8–50.2*	*Electrical (Safety) Regulations 2010 (NZ)[24]*
Australian Standards Pre-2000 2000+	*240 V 230 V +10%, −6%*	*207–253*	*49.85–50.15*	*AS 2926 (Pre-2000) [26] AS 60038-2012 Standard [27]Voltages.*

4. RESULTS AND DISCUSSION

4.1. Voltage behavior

The PV power plant injects active power and has an essential role in voltage regulation. In addition, electricity production is unsecured for renewable energy sources (due to their intermittent nature), leading to unexpected voltage fluctuations. The voltage schedule in the distribution network is determined by the consumption level and power factor of the loads. When the load changes, the voltage on the network fluctuates. The extreme case for voltage rise is a zero-consumed load associated with maximum output. Grid voltage measurements were carried out on a 9.54 kWp PV power plant installed at the UDES unit and connected to the local low-voltage grid. These measurements (as illustrated in Figure 5) display the voltage rise when the PV system is integrated into the network. Despite the increasing voltage variations, the limits of these fluctuations remain acceptable under the standard EN 50160 on the voltage characteristics of public distribution networks. The voltage quality of consumer installations is defined in the European standard EN 50160 [20]. This standard specifies a variety of quality

criteria in addition to the related limitations. It states that 95% of the voltage assessments does not exceed the specified limit. However, 5% of the values exceeding the limit are permissible. Due to the shift from the nominal voltage level of 220 V to 230 V, the upper voltage limit was set at 110% in 2008.
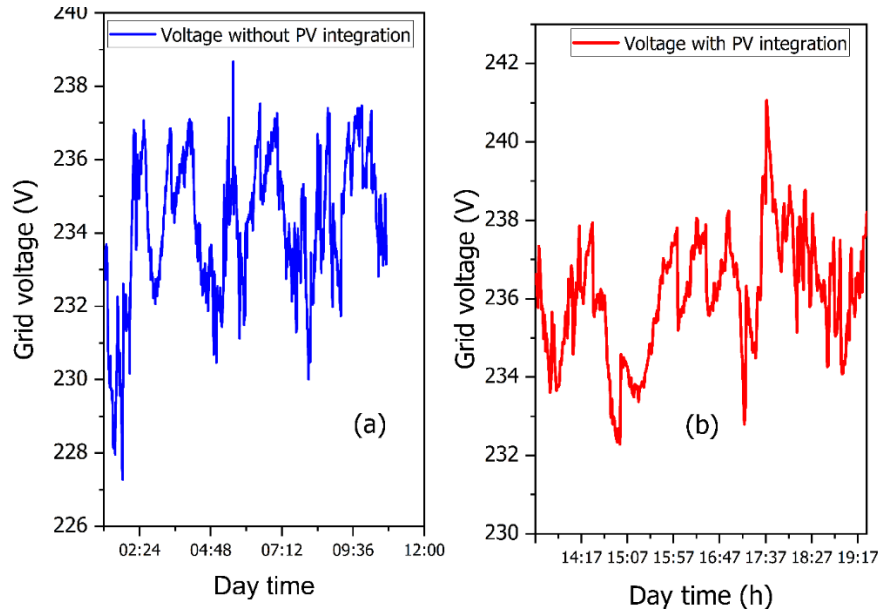

Figure 5. Increase in grid voltage with the integration of a PV power plant.

Figure 6. depicts an example of voltage distribution in relation to the lower preferred and higher operating zones defined by AS 60038. It has a Gaussian distribution around 237 V, which is 7 V higher than the nominal value. This variance is frequently permitted and remains within the limits specified by the standards AS 60038 and EN 50160. Furthermore, almost 98% of recorded voltage levels linked at the coupled point of the grid stay within the desired working range (0.98Un < Ur < 1.06Un) required by the standard AS 60038. It also reveals that more than 67% of the values are concentrated in the voltage range between 236V and 239V, reaching a peak of 21% at 237V. As a consequence of actual power injection and the system's impedance, the energy supplied by the PV panels placed in this PV power plant creates a voltage rise, notably during high solar radiation and low loads.
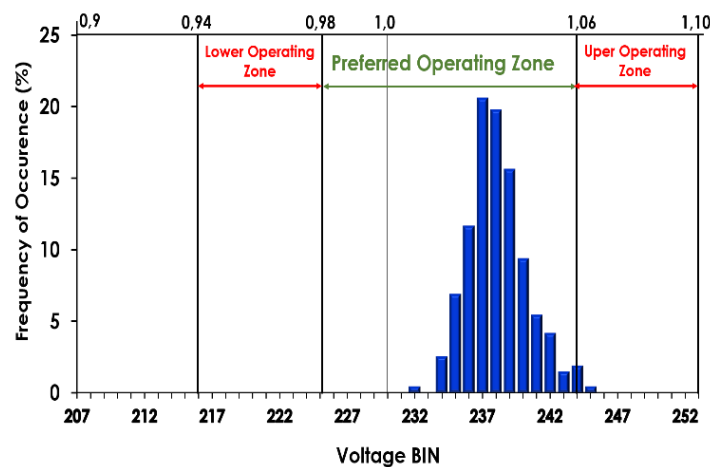

Figure 6. Voltage distribution of the PV plant's connection at the grid point based on the standard AS 61000.3.100 (230 V).

Figure 7. illustrates the relationship between the PV production output and the corresponding voltage at the grid connected point. A clear linear trend is observed, indicating that the voltage rise at the grid connected point increases proportionally with the injected active power. To better characterize this relationship, a linear regression was applied, yielding a slope, which is consistent with the theoretical model where voltage rise (ΔV) is proportional to the product of the injected power (P) and the local grid impedance (R), i.e., $\Delta V \approx R \times P$. This observation aligns with findings from previous studies, confirming that local grid impedance plays a significant role in voltage rise phenomena in low-voltage networks. Despite this increase, the measured voltage remains well within the permissible limits set by the EN 50160 standard (i.e., 230 V ±10%), indicating no adverse impact on network performance.

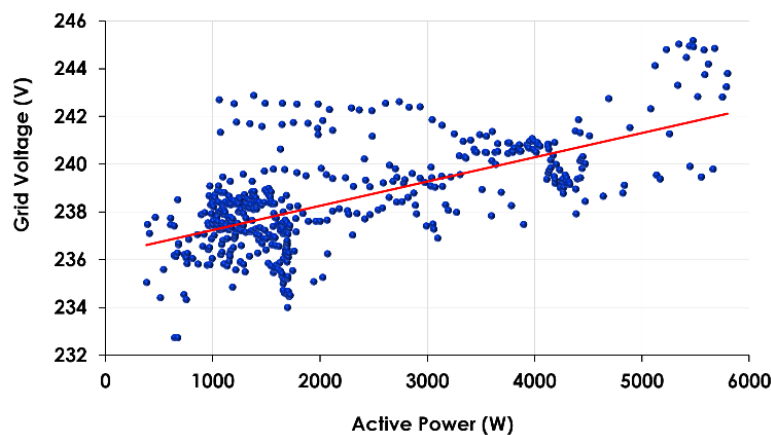Figure *7.* Grid voltage evolution as a function of the power delivered by the PV system.

4.2 Network frequency

With respect to frequency changes in the public distribution network, the standard EN 50 160 sets the limit requirements at 50 Hz 1%. Figure 8 shows the time-varying grid frequency, which demonstrates that the PV grid system meets this criteria.
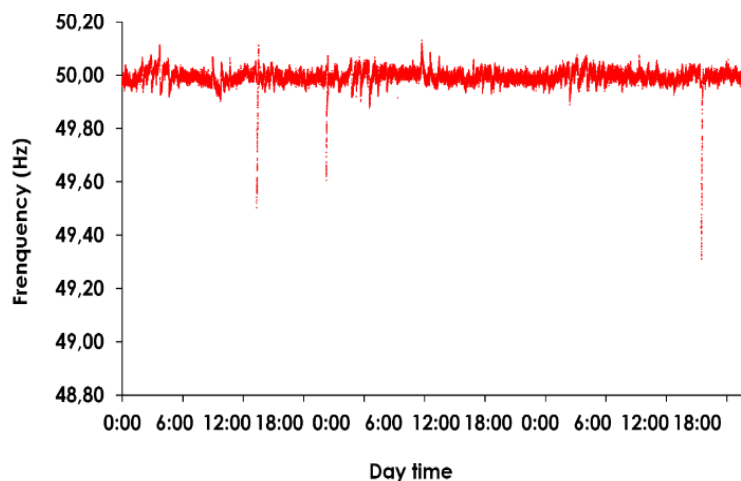

Figure 8. Grid frequency evolution in the presence of the PV

4.3 Harmonic distortion analysis

Regarding the harmonic distortion rate of current injected into the network, the results indicate a consistent decrease as the load factor increases. For load factors values exceeding 0.4 both the THD and Iac stabilize at very low levels, attaining 4.51%, 3.87% and 3.57% for low, medium and high-power levels, respectively. These values fall well within the limits prescribed

by international standards (IEC, 1995, and EN 50160). Moreover, for load factors above 0.3, the power factor converges toward unity. This trend is consistent across all three power levels, confirming that the current injected into the network is generally well regulated. At low factors, however, the power conditioning devices connected to the plant's inverters appear to lose control, resulting in increased harmonic, mainly produced by non-linear loads, can cause functional disturbances, reduced equipment life spane, and degrade overall power quality [7]. Nevertheless, inverters remain a significant source of current harmonics. Several studies have reported that inverters often operate at lower energy levels, resulting in reduced capacity to supply current at their rated power and producing a higher level of harmonics [4]. Other research[7][25] indicates that the presence of multiple inverters in a power grid can increase harmonic distortion when the inverters are of the same type. Conversely, using inverters of different types tends to reduce harmonic distortion. This behavior is related to the loss detection system in feeder grids, which, in some cases, requires measuring grid impedance by periodically injecting a current pulse and analyzing the corresponding voltage fluctuation. When identical inverters are used, this current pulse can be amplified, leading to higher harmonic distortion. Harmonics also have a direct effect on the power factor, as they contribute to reactive power generation. As the active power injected into the network increases, the power factor approaches unity. In the present case study, all of the power plant's inverters are connected to a single phase. Electrical parameters including inverter output current and voltage at the grid connection point were measured for different PV levels. The PV output was categorized into three ranges: low power (0- k KWp), medium power (0-7 KWp), and high power (0-12.5 KWp).
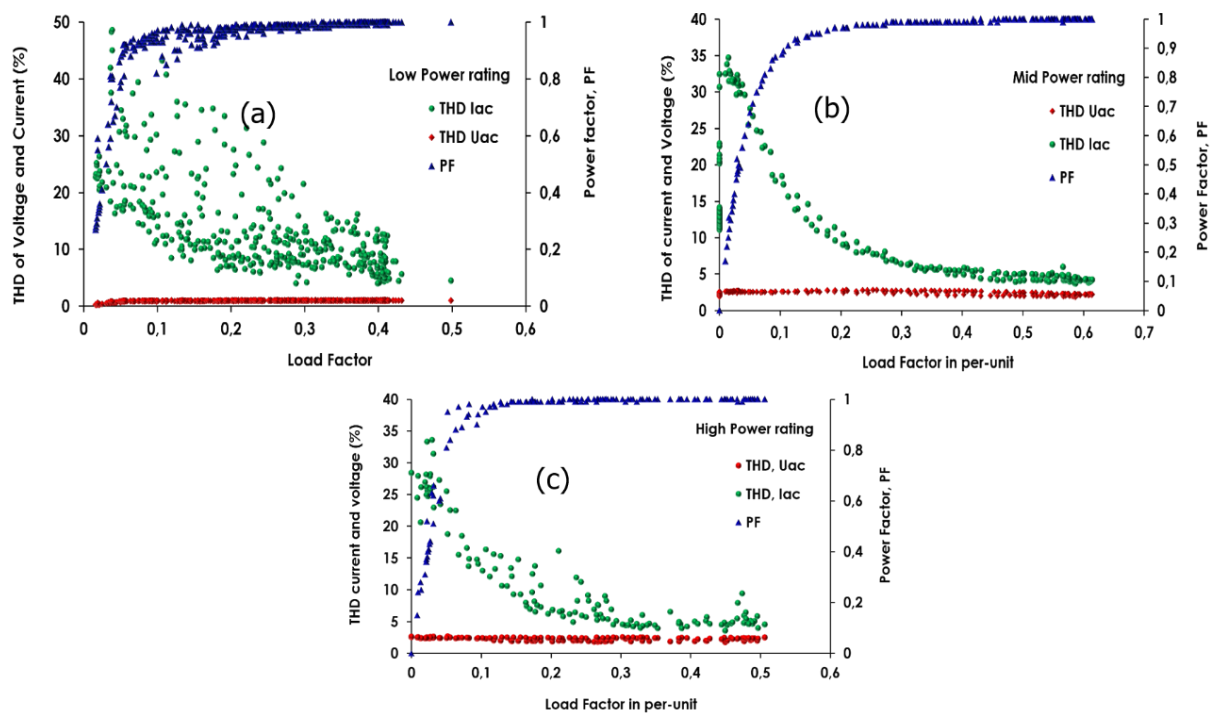

Figure 9. Harmonic distortions and power factor for: (a) low power range; (b) Medium Power Range; (c) High Power Range.

The measurement obtained in this study enabled the generation of multiple graphs illustrating the influence of PV generators on electrical network quality. The analysis focuses on current and voltage harmonics, as well as the harmonic distortion rates for both current and voltage, along with the power factor, as a function of the reduced load factor at the power generation unit. The voltage harmonic distortion values for high, medium, and low power levels re 2.26%,

2.32% and 2.42%, respectively indicating a low level of harmonics in the grid voltage waveform. When the load factor exceeds 0.4, the distortion rate stabilizes at very low levels 4.51%, 3.87%, and 3.57%for low, medium, and high-power levels, respectively fully compliant with international standard IEC (1995) and EN 50160. Furthermore, for load factors above 0.3, the power factor approaches unity. The effectiveness of current control is evident across all three power ranges; however, at low load factors, the power conditioning units connected to the plan's inverters appear to lose control of the injected current for medium and high-power ranges, more than 85% of the nominal power is injected with a distortion rate exceeds 5% for comparable production levels. Increasing active power injection into the network results in an improved load factor, with the power factor exceeding 0.95 beyond a specific threshold.

Upon examination of Figure 10, corresponding to low-, medium-, and high-power conditions, the grid voltage exhibits minimal sensitivity to variation in the injected current. Across all operating ranges, voltage fluctuations remain within narrow limits. This suggests that the low variation in voltage harmonics further confirms that the overall power quality is maintained, aligning with the compliance limits established by IEC (1995) and EN 50160 standards.
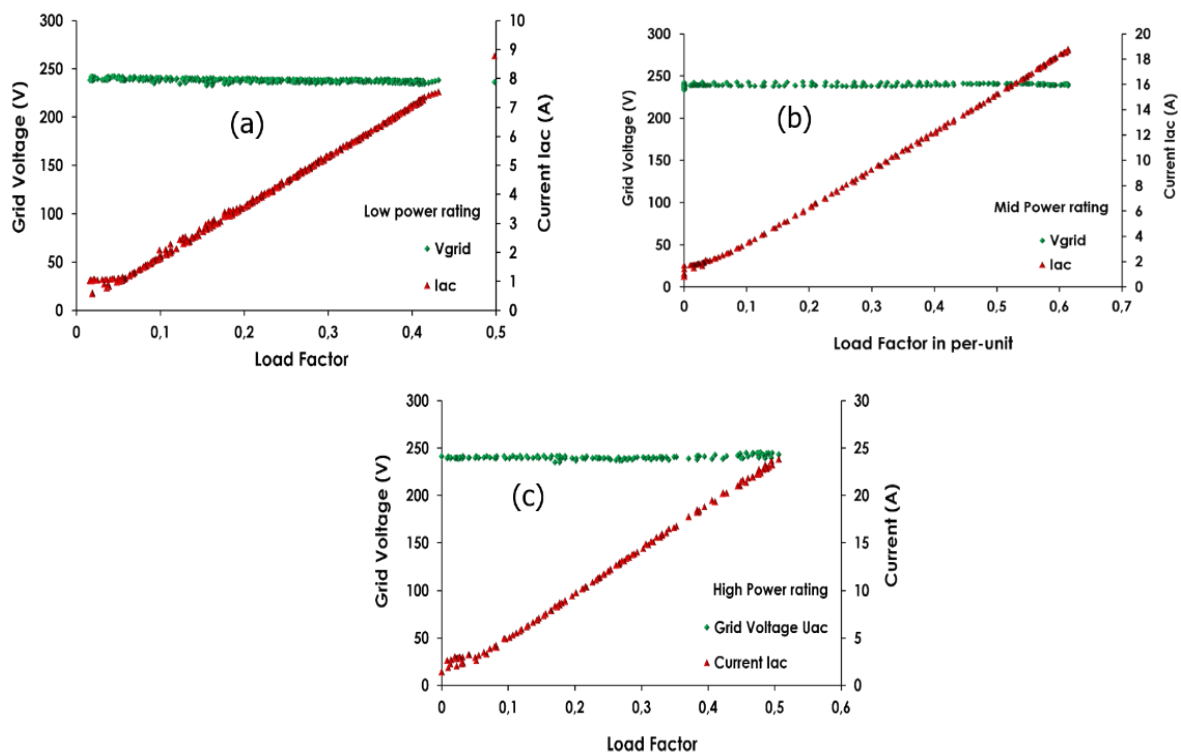

Figure 10. Efficient current values and the corresponding voltage of the PV-grid system for: (a) low power ranges; (b) medium power ranges; (c) high power ranges.
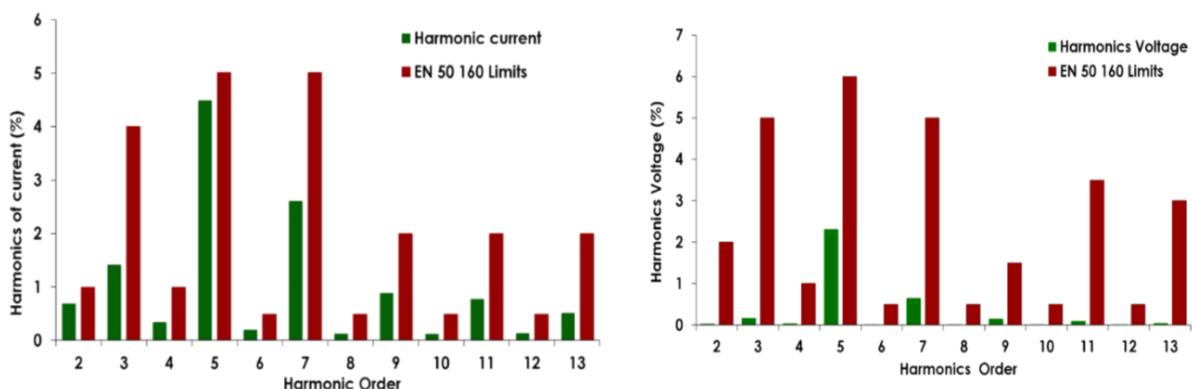

Figure 11. Description of current and voltage harmonics in relation to the EN 50160 standard limits.

Figure 11. Describe harmonic analysis of the grid injected current and voltage compared with the EN 60150 standard limits. For the injected current, all harmonic components up to order n =13 remain well below the standard limits, with the exception of the 5 th and 7 th order harmonics slightly exceed 1%; except for the 5 th order harmonics, which reaches approximately 2% still significantly below the EN 50160 limit of 6%.

4.4. Grid compliance and implications

To perform a detailed analysis of the impact of the PV energy on the low-voltage distribution network, simulations were carried out for the three previously considered power ranges over a one-day period. The PV production profile was analyzed alongside the current THD injected into the grid. as shown in Figure 12, the current THD decrease during PV system operation, whereas for night times periods (without PV generation), increase again. This rise at night occurs because, in the absence of PV injection, the current in the network is supplied entirely by other connected loads many of which are nonlinear devices that introduce higher harmonic currents. In contrast, during the day, the PV system injects a near sinusoidal current into the grid, which effectively dilutes the distortion from other loads and lowers the overall THD. Furthermore, it is evident that the THD of the alternating current Iac exhibits elevated levels exclusively during sunrise and sunset. Through the daytime, the current THD remain consistently low, with fluctuations below 5%. The Figures represented in this study highlight the considerable variations in PV production, particularly on partially cloudy days, which cause noticeable change in the current THD values. Conversely, on clear days like (Figure 12b), there is a close correlation between PV production and solar irradiation patterns, resulting in a stable and low harmonic distortion rate throughout the day.
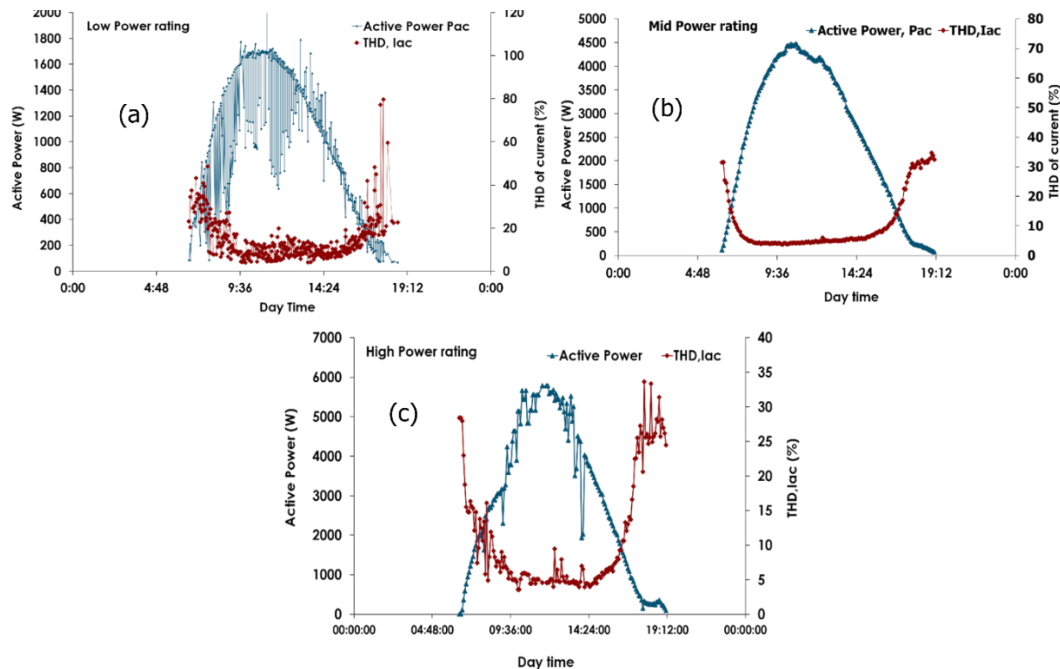

Figure 12. Evolution of the current in PV production's harmonic distortion rate for: (a) low power ranges; (b) medium power ranges; (c) high power ranges.

As shown in Figure 13, fluctuation in PV production particularly pronounced during intermittent cloud cover lead to rapid variations in the power injected into the grid. These variations result in important fluctuations in the distribution network. Such effects are

particularly visible in low- voltage systems with limited load capacity, where unexpected change in PV output can cause *localized voltage instability. In contrast, throughout periods of stable solar irradiance, active power injection remains steady, and the related grid voltage profile exhibits minimal oscillations.*
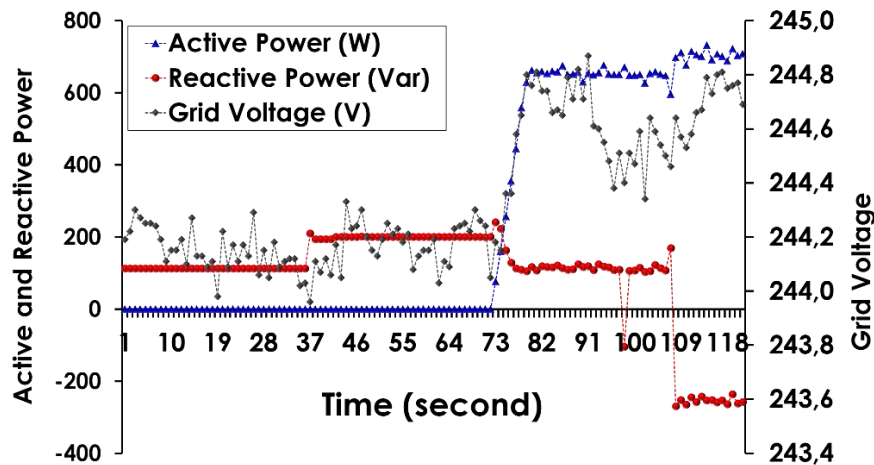

Figure 13. Evolution of power and grid voltage during the PV power injection into the grid.

4.5 Statistical Analysis

To provide deeper insight into the beneficial effects of integrating photovoltaic systems into the conventional power grid, statistical analyses were carried out on key power quality indicators. Specifically, histograms (Figures 14, 15, and 16) were constructed to illustrate the frequency distribution of current total harmonic distortion), voltage total harmonic distortion, and power factor values under three distinct levels of photovoltaic power generation. Each histogram was fitted with a normal distribution curve, defined by its mean value and standard deviation, enabling a clear visualization of both the central tendency and the dispersion of the measured data. This approach not only facilitates comparison between operating conditions but also highlights how variations in PV output influence the statistical behavior of these critical parameters. Figure 14 shows the histograms of current THD, voltage THD, and power factor for the low PV power range, overlaid with fitted normal distribution curves indicating the mean and standard deviation.
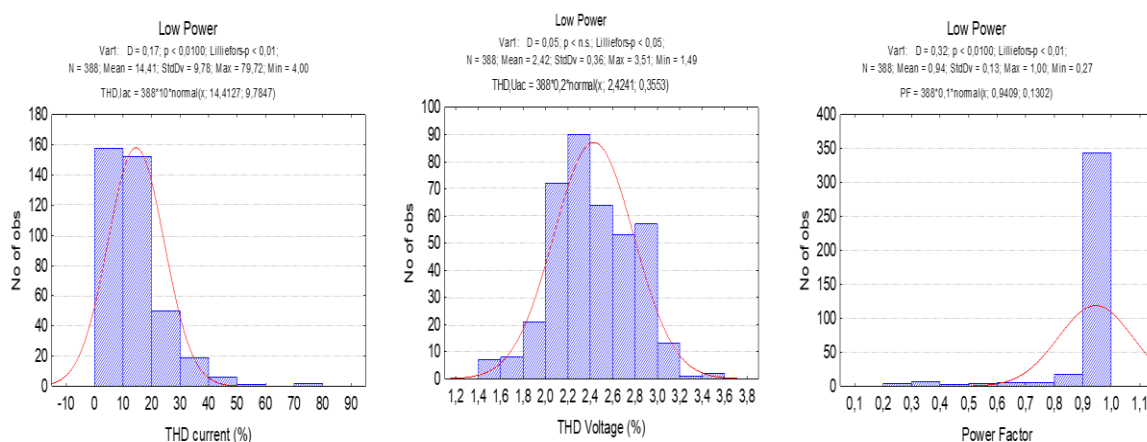

Figure 14. Histogram of current and voltage THD and power factor, with a normal distribution fit showing the mean and standard deviation (low power range).

Figure 15 depicts the histograms of current THD, voltage THD, and power factor for the medium PV power range, overlaid with fitted normal distribution curves indicating the mean
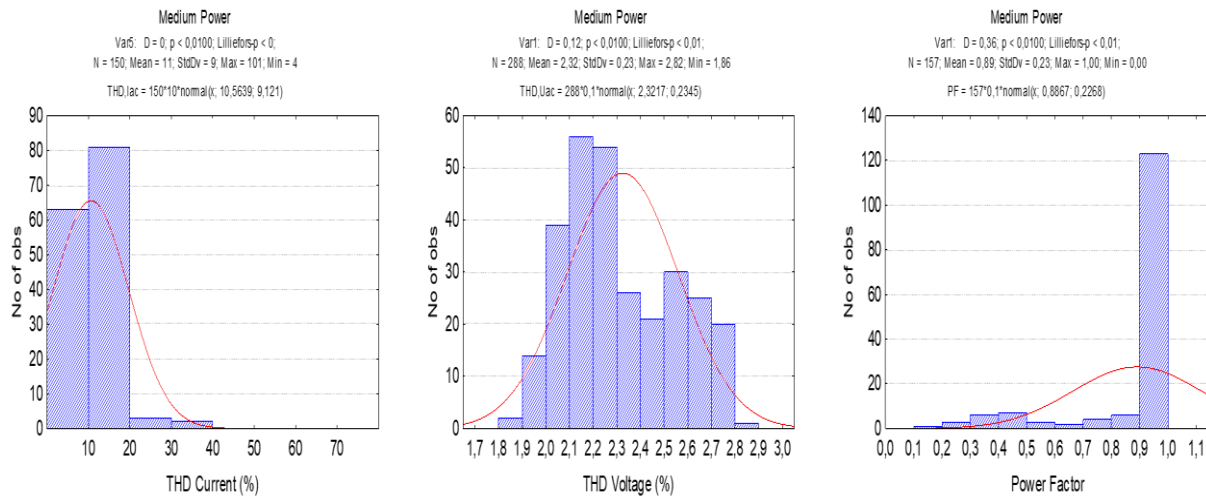
and standard deviation.

Figure 15. Histogram of current and voltage THD and power factor, with a normal distribution fit showing the mean and standard deviation (medium power range).

Figure 16 depicts the histograms of current THD, voltage THD, and power factor for the high PV power range, overlaid with fitted normal distribution curves indicating the mean and standard deviation.
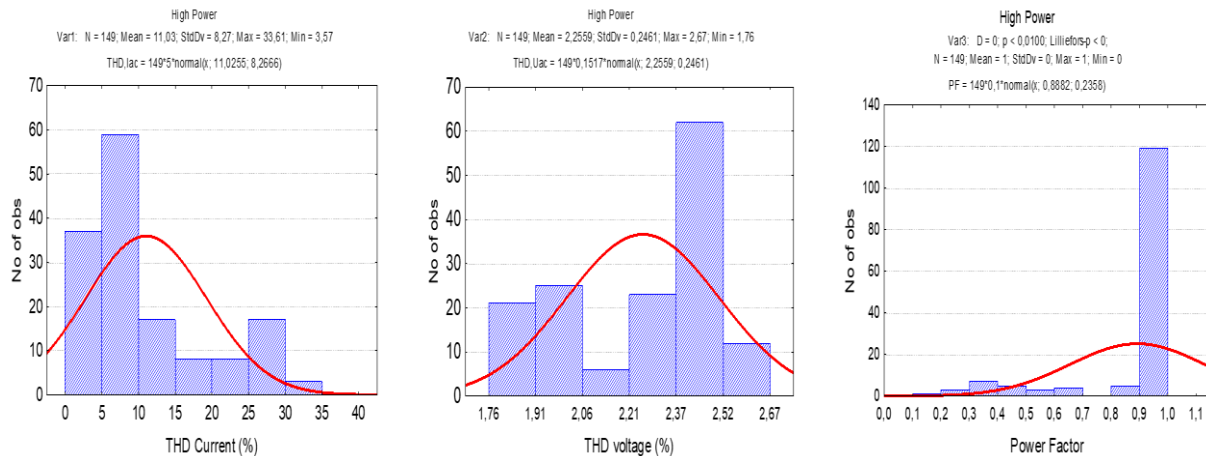

Figure 16. Histogram of current and voltage THD and power factor, with a normal distribution fit showing the mean and standard deviation (high power range).

Several observations were made concerning both how these variables are distributed relative to the limits set by the EN 15160 and IEC 61000-4-30 standards, and how their values cluster around the mean estimated from the fitted normal distribution. Although all measured current THD values are significantly below the limit specified by the EN 15160 standard, the data reveal that more than 80% of these values are concentrated within the 5%–10% range. Furthermore, the standard deviation decreases from 9.78 to 8.23 as photovoltaic output increases, resulting in a narrower and more pronounced normal distribution, indicative of reduced variability in current distortion under higher generation conditions. A comparable trend is observed for voltage THD: as photovoltaic production rises, the mean value of the distribution decreases from 2.42 to 2.26, reflecting an overall improvement in voltage waveform quality. Notably, more than 96% of the measured voltage THD values lie well below the EN 15160 compliance

threshold, confirming the minimal harmonic impact of the PV system on the grid. As for the power factor, results clearly show that, across all three PV output levels, over 80% of the measured values are clustered close to unity. This high concentration near the optimal value indicates efficient real power transfer and minimal reactive power exchange between the PV system and the utility grid, even under varying generation conditions.

5. CONCLUSION

This study presented a detailed experimental assessment of a 12.5 kWp multi-technology photovoltaic power plant connected to the low-voltage grid at the UDES unit in Tipaza, Algeria. The system, comprising five PV arrays with different technologies and orientations, was monitored under real operating conditions to evaluate its impact on voltage stability, harmonic distortion, and power factor. Results showed that voltage variation at the grid-connected point consistently remained within EN 50160 limits, with deviations not exceeding ±5% even during peak PV injection. Statistical analysis of harmonic distortion revealed that more than 85% of the energy produced under high irradiance conditions was injected with current THD values below 5%, in full compliance with IEC 61000-3-2 requirements. Higher current THD values were observed primarily at low power injection levels, confirming a power-law relationship between output power and distortion. The standard deviation of current THD decreased from 9.78 to 8.23 as PV output increased, indicating a more concentrated and stable distribution at higher generation levels. For voltage THD, the mean value decreased from 2.42 to 2.26 as PV production rose, and more than 96% of recorded values were well below the EN 15160 limit, confirming minimal harmonic impact on the grid. The power factor remained high across all operating conditions, with over 80% of values clustered near unity, reflecting efficient real power transfer and limited reactive power exchange. These results collectively demonstrate that the inverters provided effective voltage regulation and maintained high power quality, even under variable generation. The findings confirm that small-scale PV systems in the kWp range, when properly configured and managed, are technically compatible with low-voltage distribution grids and can actively support decentralized energy strategies without compromising grid stability or power quality. Nevertheless, the study is limited to an installation operating under specific local grid conditions, and its moderate capacity does not capture potential interactions in high-penetration scenarios. Furthermore, the inability to scale the system beyond 12.5 kWp or simulate higher injection capacities restricted the scope of the analysis.

REFERENCES

[1]   *"What Is Iea Pvps," pp. 1–16, 2015.*

[2]   *"MODEL FORMS Usage and Reproduction of IET Forms," no. July, 2015.*

[3]   A. Honrubia-Escribano, A. Molina-Garcia, E. Gomez-Lazaro, and E. Muljadi, "Power quality survey of a photovoltaic power plant," *Conf. Rec. IEEE Photovolt. Spec. Conf.*, pp. 1799–1804, 2013, doi: 10.1109/PVSC.2013.6744492.

[4]   A. Canova, L. Giaccone, F. Spertino, and M. Tartaglia, "Electrical impact of photovoltaic plant in distributed network," *IEEE Trans. Ind. Appl.*, vol. 45, no. 1, pp. 341–347, 2009, doi: 10.1109/TIA.2009.2009726.

[5]   V. R. F. B. De Souza, M. A. Filho, and K. C. De Oliveira, "Analysis of power quality for photovoltaic systems connected to the grid," *Proc. Int. Conf. Harmon. Qual. Power, ICHQP*, vol. 2016-Decem, no. 5, pp. 226–230, 2016, doi: 10.1109/ICHQP.2016.7783418.

[6]   P. González, E. Romero-Cadaval, E. González, and M. A. Guerrero, "Impact of grid connected photovoltaic system in the power quality of a distribution network," *IFIP Adv. Inf. Commun. Technol.*, vol. 349 AICT, pp. 466–473, 2011, doi: 10.1007/978-3-642-19170-1_51.

[7]   S. M. Ahsan, H. A. Khan, A. Hussain, S. Tariq, and N. A. Zaffar, "Harmonic analysis of grid-connected solar PV systems with nonlinear household loads in low-voltage distribution networks," *Sustain.*, vol. 13, no. 7, 2021, doi: 10.3390/su13073709.

[8]   I. Kim and M. Begovic, "On impact of randomly distributed PV systems on distribution networks," *Proc. Annu. Hawaii Int. Conf. Syst. Sci.*, vol. 2016-March, no. February, pp. 2418–2425, 2016, doi: 10.1109/HICSS.2016.302.

[9]   M. J.-E. Alam, "Grid integration of solar photovoltaic resources: impact analysis and mitigation strategies," p. 222, 2014, [Online]. Available: http://ro.uow.edu.au/theses/

[10]   M. Maghalseh, N. Iqteit, H. Alqadi, and S. Ajib, "Investigation of Grid-Tied Photovoltaic Power Plant on Medium-Voltage Feeder: Palestine Polytechnic University Case Study," *Solar*, vol. 5, no. 1, 2025, doi: 10.3390/solar5010001.

[11]   OBSERVATOIRE GÉOSTRATÉGIQUE DU SPORT, "Du Sport Impact De La Mondialisation Sur Le Sport : Impact De La Mondialisation Sur Le Sport," no. December 2017, 2015.

[12]   M. Mourad Mabrook, A. A. Donkol, A. M. Mabrouk, A. I. Hussein, and M. Barakat, "Enhanced the Hosting Capacity of a Photovoltaic Solar System Through the Utilization of a Model Predictive Controller," *IEEE Access*, vol. 12, no. January, pp. 62480–62491, 2024, doi: 10.1109/ACCESS.2024.3392645.

[13]   F. Peprah, S. Gyamfi, M. Amo-Boateng, and E. Effah-Donyina, "Impact assessment of grid tied rooftop PV systems on LV distribution network," *Sci. African*, vol. 16, no. April, p. e01172, 2022, doi: 10.1016/j.sciaf.2022.e01172.

[14]   P. Phukpattaranont, M. S. Janthong, and P. Phukpattaranont, "Grid-Connected

Residential PV Systems: Assessing Power Quality Disturbance Impacts," no. December, 2024, [Online]. Available: https://www.researchgate.net/publication/387292214

[15] *C. Gandikoti, S. K. Jha, B. M. Jha, and P. Mishra, "Distributed voltage unbalance mitigation in islanded microgrid using moth flame optimization and firebug swarm optimization," Int. J. Power Electron. Drive Syst., vol. 15, no. 2, pp. 824–834, 2024, doi: 10.11591/ijpeds.v15.i2.pp824-834.*

[16] *M. Værbak, J. D. Billanes, B. N. Jørgensen, and Z. Ma, "A Digital Twin Framework for Simulating Distributed Energy Resources in Distribution Grids," Energies , vol. 17, no. 11, 2024, doi: 10.3390/en17112503.*

[17] *L. E. S. e. Silva et al., "Probabilistic operational costs assessment of combined PV–PEV connections in LV distribution networks," Electr. Power Syst. Res., vol. 214, no. PB, p. 108906, 2023, doi: 10.1016/j.epsr.2022.108906.*

[18] *EN 50160, "Voltage characteristics of electricity supplied by public electricity networks," Eur. Comm. Electrotech. Stand., vol. 33, no. 0, 2010.*

[19] *ISO 5167-2:2003(E), "International Standard IEC 61000-4-30," 61010-1 © Iec2001, vol. 2003, p. 13, 2021.*

[20] *EN 50160, "Voltage characteristics of electricity supplied by public electricity networks," Eur. Comm. Electrotech. Stand., 2010.*

[21] *S. Australia, "Australian Standard ^{TM} Standard Voltages IEC60038:1983," pp. 5–9, 2000, [Online]. Available: www.standards.com.au*

[22] *BSI, "Requirements for electrical installations," IET wiring Regul. 18th Ed., vol. 2, no. 2, p. 560, 2018.*

[23] *ANSI Standard Publication, "American National Standard for Electric Power Systems and Equipment-Voltage Ratings(60Hertz)," ANSI Stand Z17. 1, no. March 10, pp. 1–7, 2020.*

[24] *A. Satyanand, "Electricity (Safety) Regulations 2010 Order in Council," 2010.*

[25] *N. Anang and W. M. W. Muda, "Analysis of total harmonic distortion in single-phase single-stage grid-connected photovoltaic system," Int. J. Power Electron. Drive Syst., vol. 14, no. 1, pp. 471–479, 2023, doi: 10.11591/ijpeds.v14.i1.pp471-479.*

[26] *Standards Association of Australia, AS 2926 — Standard Voltages, Standards Association of Australia, Sydney, Australia, 1987.*

[27] *Standards Australia, AS 60038-2012 — Standard Voltages, Standards Australia International Ltd., Sydney, Australia, 2012.*